ARTICLES SCIENCE CHINA Materials

mater.scichina.com link.springer.com

Published online 12 January 2018 | https://doi.org/10.1007/s40843-017-9177-5

Sci China Mater 2018, 61(2): 254–262

SPECIAL ISSUE: Innovative Electrode Materials for Supercapacitors

Self-healable wire-shaped supercapacitors with two twisted $NiCo_2O_4$ coated polyvinyl alcohol hydrogel fibers

Rui Jia[1,2†], La Li[2†], Yuanfei Ai[2], Hui Du[1], Xiaodong Zhang[1], Zhaojun Chen[1*] and Guozhen Shen[2,3*]

ABSTRACT **Wire-shaped supercapacitors (SCs) possessing light-weight, good flexibility and weavability have caught much attention, but it is still a challenge to extend the lifespan of the devices with gradual aging due to the rough usage or external factors. Herein, we report a new stretchable and self-healable wire-shaped SC. In the typical process, two polyvinyl alcohol/potassium hydroxide (PVA/KOH) hydrogel wrapped with urchin-like $NiCo_2O_4$ nanomaterials were twisted together to form a complete SC devices. It is noted that the as-prepared PVA hydrogel can be easily stretched up to 300% with small tensile stress of 12.51 kPa, superior to nearly 350 kPa at 300% strain of the polyurethane. Moreover, the wire-like SCs exhibit excellent electrochemical performance with areal capacitance of 3.88 mF cm^{-2} at the current density of 0.053 mA cm^{-2}, good cycling stability maintaining 88.23% after 1000 charge/discharge cycles, and 82.19% capacitance retention even after four damaging/healing cycles. These results indicate that wire-shaped SCs with two twisted $NiCo_2O_4$ coated polyvinyl alcohol hydrogel fibers is a promising structure for achieving the goal of high stability and long-life time. This work may provide a new solution for new generation of self-healable and wearable electronic devices.**

Keywords: supercapacitors, self-healable, nanowires, flexible electronics

INTRODUCTION

The rapid developing wearable electronic devices have gained increasing attention for their widely application in the fields of wearable watch, portable cellphone and drug testing devices [1–9]. Recently, one-dimensional (1D) electronic devices have become new generation of wearable devices that could be integrated with intelligent clothing easily [10–13]. However, most of the wearable 1D electronic devices tend to be cracked microcosmically due to human activities and many other external forces, which will lead to the performance degradation and even invalidation of the whole device [14,15]. Therefore, new kinds of self-healing electronic devices are still urgently needed for their potential application in the field of self-healing energy storage, self-healing detectors and self-healing sensors [16,17].

In particular, the self-healing supercapacitor (SC) is regarded as a promising candidate for self-healable energy storage devices because of their high compatibility with other wearable devices, high power/energy density compared with traditional capacitor and batteries, and excellent mechanical electrical recovery performance [18–21]. Currently, most of the materials of self-healing SCs are focused on polyurethane (PU) or polymer synthesized by chemical methods. As the previous reports, Gao's group designed reduced graphene oxide fiber SCs wrapped by PU to ensure recovering the broken surface [22]. Chen's group fabricated a kind of self-healing SC through synthesizing the polymer of supramolecules cross-linked with TiO_2 nanospheres by hydrogen bond [23]. Nevertheless, the PU and the synthesized polymer cannot be separated in the complex chemical synthesis procedure. To overcome this problem, Wei *et al.* [24] proposed that polyvinyl alcohol (PVA) can be cross-linked to network by adding glutaraldehyde. However, adding cross-linking agent to obtain the stretching and self-healing PVA

[1] College of Chemistry and Chemical Engineering, Qingdao University, Qingdao 266071, China
[2] State Key Laboratory for Superlattices and Microstructures, Institute of Semiconductors, Chinese Academy of Sciences, Beijing 100083, China
[3] College of Materials Science and Opto-electronic Technology, University of Chinese Academy of Sciences, Beijing 100049, China
[†] These two authors contributed equally to this work.
[*] Corresponding authors (emails: chenzj_upc@126.com (Chen Z); gzshen@semi.ac.cn (Shen G))

substrate is not an environmentally friendly solution.

Here, we report a wire-shaped supercapacitor with excellent stretching performance and self-healing stability by twisting two urchin-like $NiCo_2O_4$ nanomaterials coated PVA/KOH hydrogel. The synthesized urchin-like $NiCo_2O_4$ nanostructures with the "V-type" channels can reduce the ion-transport resistance and diffusion distance from the outer electrolyte to the inside surfaces, resulting in better electrochemical performance [25–27]. The PVA/KOH hydrogel fiber substrate can be easily stretched to 300% with smaller tensile stress of 12.51 kPa and realize automatic self-healing of broken area once the supercapacitor suffers to damage. The assembled devices exhibit excellent electrochemical properties and high mechanical stability, providing a long lifespan model for 1D self-healable wearable electronic device in the future.

EXPERIMENTAL SECTION

Materials synthesis

PVA/KOH gel electrolyte polymer was obtained according to our previous reports [28–31]. Briefly, 3 g of PVA were added in 28 mL of deionized (DI) water with stirring at 98°C for 1 h. Then, 1.68 g of KOH were dissolved in 2 mL of DI water. The KOH solution was then dropped into the viscous PVA solution under stirring to get a clear solution. PVA with low-molecular-weight (molecular weight from 63,800 to 114,400) and high-molecular-weight (molecular weight from 118,756 to 123,200) were prepared with the same method, respectively.

Urchin-like $NiCo_2O_4$ nanostructures were synthesized *via* a hydrothermal route. Typically, 0.72 mmol $Ni(NO_3)_2{\cdot}6H_2O$, 1.48 mmol $Co(NO_3)_2{\cdot}6H_2O$, and 0.6 g urea were dissolved in 30 mL DI water under constant stirring, respectively. Then the solution was transferred into a Teflon-lined stainless autoclave and heated at 110°C for 12 h. When the autoclave was cooled down to room temperature, the precipitate was collected and washed with DI water and ethanol for several times, and dried in vacuum oven at 60°C for 12 h. Finally, the precipitate was annealed at 400°C under air for 3 h.

Fabrication of self-healing SC devices.

To fabricate wire-like supercapacitor devices, silicone pipes with diameter of 2 mm and length of 1.5 cm were first prepared. Then, high-molecular-weight PVA/KOH hydrogel was injected into the pipes, which were put into refrigerator to obtain gel-type PVA/KOH hydrogel fibers by circulating frozen at −4°C [32]. After that, the hydrogel fibers were drawn out from the silicon pipe gently. The $NiCo_2O_4$ slurry was prepared by mixing the $NiCo_2O_4$ nanomaterials and polyvinylidene fluoride (PVDF) at a mass ratio of 9:1 with 99.5 wt.% ethanol. Following, the $NiCo_2O_4$ materials were brushed onto the hydrogel fibers with a brush pen at gently stretching state and then the low-molecular-weight PVA/KOH electrolyte was coated on the surface of the above hydrogel fibers to form the electrodes. The electrical resistance of the electrode is about 600 Ω measured by the multimeter. Eventually, two PVA/KOH hydrogel fibers were twisted together for about four loops to fabricate the symmetric supercapacitor devices. The surface area (S) of the electrode is calculated with the equation: $S=\pi dL$, where d is the diameter of the electrode (cm) and L is the length of the electrode covered with electrolyte (cm).

Characterizations.

X-ray diffraction (XRD) measurements were performed through an instrument of Bruker D8 Advance X-Ray diffractometer with radiation from a Cu target (Kα, λ =0.15406 nm). Scanning electron microscopy (SEM) tests were carried out to examine the surface morphology of the products using an equipment of NanoSEM650-6700F with a voltage of 5 kV. Transmission electron microscopy (TEM) characterization was performed using an instrument of JEOLJEM-2010HT with a voltage of 200 kV. The CHI 760D electrochemical work station was used to measure the electrochemical properties of the fabricated wire-like SCs.

RESULTS AND DISCUSSION

Fig. 1 shows the photographs and physical properties of the synthesized PVA/KOH hydrogel fiber obtained from the circulating frozen process. As shown in Fig. 1a, the diameter of the PVA/KOH hydrogel fiber is about 2 mm and the pristine length is 1.5 cm. Using 1D platform, the hydrogel fiber can be stretched from 1.5 cm to 6 cm. That is, the excellent stretchability up to 300% has been demonstrated in the hydrogel fiber. The stretched hydrogel fiber can be easily twisted onto the thumb as shown in upper right Fig. 1a, which suggests it is a potential candidate for stretchable fiber substrate in wearable electronics. The self-healing properties of the hydrogel fiber were then measured by cutting it into halves using a scalpel. Subsequently, the two broken areas were brought into contact with each other under a gentle pressure and several drops of water were dropped to promote the self-healing process at the same time. About ten minutes later, the internal contacted two broken fibers successfully blended together. Fig. 1b shows the photographs of the

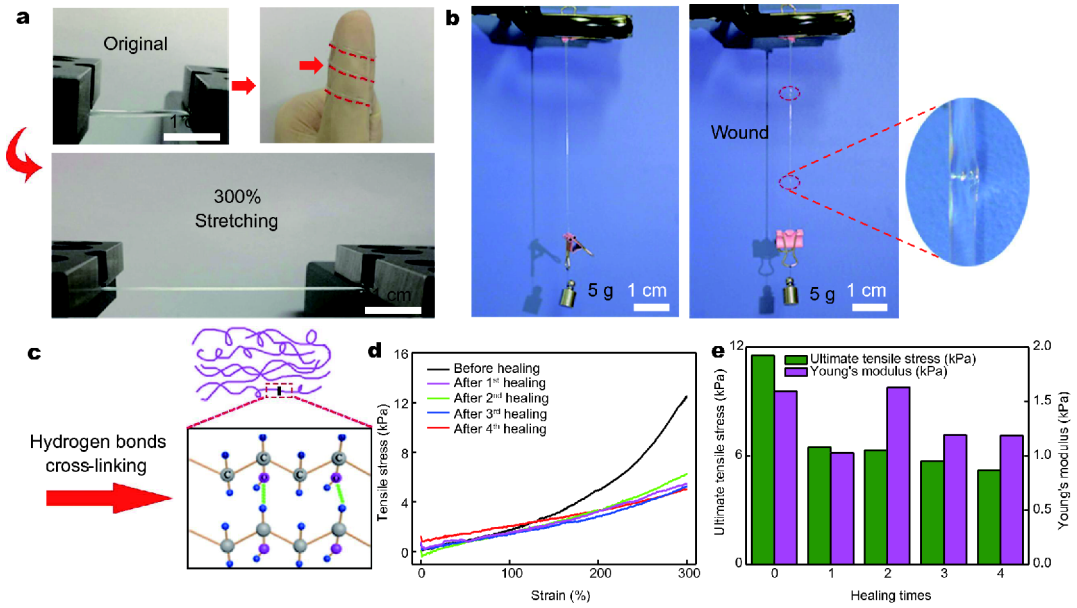

Figure 1 (a) Optical images of the stretchable PVA/KOH hydrogel: stretching from 1.5 to 6 cm by employing one-dimensional platform (left) and twisting on the thumb (upper right). (b) Illustration of the PVA/KOH hydrogel to support a 5 g mass: before damaging (left), after healing (right) and magnified image of the wound positions. (c) Schematic plot of the self-healing mechanism. (d) Tensile tests of the PVA/KOH hydrogel fiber after different damaging/healing cycles. (e) Tensile strengths and Young's modulus of the PVA/KOH hydrogel fiber after different damaging/healing cycles.

pristine and the self-healed hydrogel fibers supporting a 5 g mass, respectively, which reveals that the stretchable hydrogel fiber has superior self-healing performance at room temperature. The magnified picture in Fig. 1b shows the self-healed positions after the recombination of supramolecules. It is noted that no obvious crack was observed in the wound position, which indicates that the self-healing phenomenon in this material is not a simple adhesion effect. The remarkable stretching and self-healing behaviors are attributed to the chains and cross-links *via* intermolecular hydrogen bonds, as displayed in Fig. 1c. The tensile measurements and Young's modulus of the PVA/KOH fiber after different cutting/self-healing cycles were then investigated in detail using the tensile machine (as shown in Fig. 1d and e). From the Fig. 1d, it is clear that the tensile stress reached 12.5 kPa when the stretching elongation increased to 300%, which is almost 30 orders of magnitude smaller than that of PU under the same level of stretch. All these results demonstrate the excellent tensile properties of the as-prepared PVA hydrogel [33]. Moreover, as showed in Fig. 1e, the tensile stress gradually decreases after the first healing process, and almost becomes invariably in the subsequent three healing cycles. After the fourth healing, the Young's modulus of the as-prepared PVA hydrogel remains 74.29% of the initial value.

The morphology and microstructure of the as-obtained $NiCo_2O_4$ samples were characterized by SEM and TEM. Fig. 2a shows the SEM images of the annealed product, where the urchin-like samples with an average length of 3 μm have been prepared using hydrothermal method. The enlarged view of SEM image showed in Fig. 2b indicates that the urchin-like products consist of numerous nanorods grown from the center. The diameter of the nanorods is ranging from 100 to 200 nm, which is consistent with our previous reports [34,35]. Furthermore, the TEM images (Fig. 2c and d) with different magnifications also reveal the same morphology and diameter, in agreement with the SEM images. Fig. 2e shows the high-resolution TEM (HRTEM) image of $NiCo_2O_4$ nanorod. The clearly resolved lattice fringes of 0.24 and 0.28 nm correspond well to the (311) and (220) facets of the spinel structured $NiCo_2O_4$, which indicates the polycrystalline structure of $NiCo_2O_4$ nanorods. The inset figure shows the selected area electron diffraction (SAED) pattern of the $NiCo_2O_4$ electrode materials. In addition, the Fig. 2f exhibits the XRD pattern of $NiCo_2O_4$. All the peaks are in consistent with the standard pattern of the $NiCo_2O_4$ (JCPDS 20-0781). No other peaks are found, which suggests the high quality of the prepared $NiCo_2O_4$ electrode materials.

To take advantage of the excellent stability/stretch-

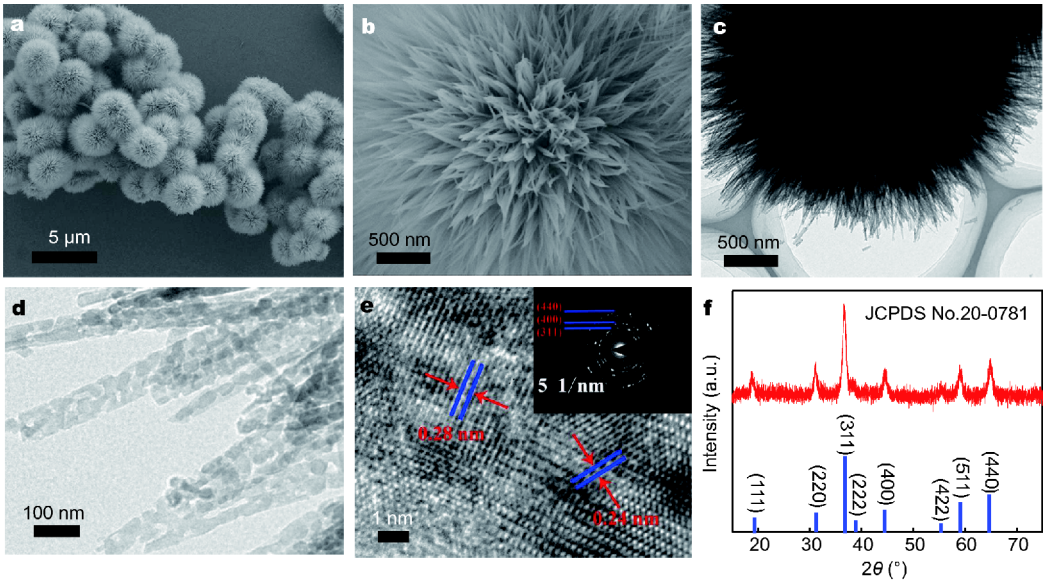

Figure 2 (a, b) SEM images, (c, d) TEM images, (e) HRTEM image and (f) XRD pattern of the obtained urchin-like $NiCo_2O_4$ nanostructures.

ability of the PVA fiber substrate with high-molecular-weight and good conductivity of the $NiCo_2O_4$ electrode materials (Fig. S1, Supplementary information), we then fabricated all solid-state wire-like SCs in PVA/KOH gel electrolyte. The electrochemical performance of the as-prepared urchin-like $NiCo_2O_4$ nanostructures was first measured in a three-electrode system in 3.0 mol L^{-1} KOH aqueous electrolyte (Fig. S2). It is noted that the as-prepared urchin-like $NiCo_2O_4$ nanostructures exhibited a specific capacitance of 641 F g^{-1} at the scan of 5 mV s^{-1}, as well as excellent cycling stability with capacitance retention of 95% after 5,000 cycles. All-solid-state wire-like SCs were then fabricated and tested under the two-electrode system. The urchin-like $NiCo_2O_4$ samples were uniformly covered on the PVA/KOH hydrogel fiber, serving as both cathode and anode materials. Besides, SEM image was provided to show the distribution of $NiCo_2O_4$ nanostructures mixed with PVDF at the mass ratio of 9:1 on the PVA hydrogel (Fig. S3), which demonstrates the tight contact between $NiCo_2O_4$ crystals and the PVA hydrogel. Then, the assembled SC was shown in the inset of Fig. 3f. Fig. 3a shows the cyclic voltammetry (CV) curves of the device, which is measured at the scan rates ranging from 0.1 to 3.0 V s^{-1} and the potential window ranging from 0 to 0.8 V. The current is clearly increased as the scan rate increased, confirming the typical faradaic pseudocapacitive behavior of the wire-like SCs. The galvanostatic charge-discharge (GCD) measurements of the wire-like SCs were also performed at different current densities of 0.053, 0.085, 0.096, 0.106, 0.212 and 0.319 mA cm^{-2}, as displayed in Fig. 3b. All the GCD curves present relative symmetric triangular shapes, showing the outstanding Coulombic efficiency of the fabricated SCs devices. Here, the capacitances were calculated based on the GCD curves and the results are shown in Fig. 3c. It is noted that the areal capacitance of the device can reach 3.88 mF cm^{-2} at the current density of 0.053 mA cm^{-2}, which is much higher than the previously reported values of wire-like SCs [36–38]. Furthermore, the areal capacitance of the fabricated device remains at 1.18 mF cm^{-2} even the current density increases to 0.319 mA cm^{-2}, which indicates the good rate capability of the assembled wire-like SCs. Fig. 3d presents the electrochemical impedance spectroscopy (EIS) of the wire-like SCs in frequencies varying from 100 KHz to 0.01 Hz. The Nyquist plots represent the charge transport resistance of 20.5 Ω. Besides, the long-term cycling performance of the wire-like SCs was conducted for 1000 cycles at a charge-discharge rate of 0.425 mA cm^{-2}. As shown in Fig. 3e, the wire-like SC device exhibits outstanding stability with the cycle retention of 88.23% of the initial capacitance after 1000 cycles. Fig. 3f shows the maximum areal energy density calculated to be about 0.338 μW h cm^{-2} at the power density of 20 μW cm^{-2}. The excellent performance of the wire-like SC can be explained from the urchin-like $NiCo_2O_4$ nanostructures with the "V-type" channels, which could reduce the ion-transport resistance, shorten the diffusion distance, and increase the utilization of the electrode materials.

The stretchable performance of the wire-like SCs at

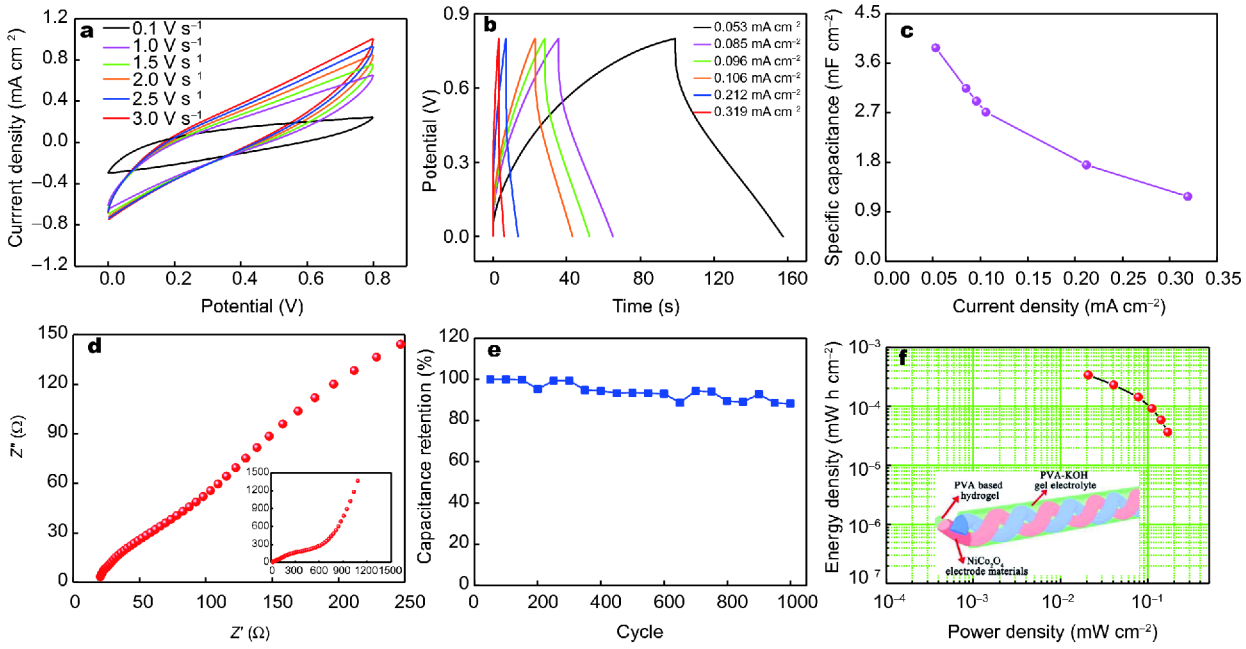

Figure 3 Electrochemical performance of the fabricated wire-like SCs with urchin-like $NiCo_2O_4$ electrodes. (a) CV curves at different scan rates ranging from 0.1 to 3.0 V s^{-1}. (b) GCD curves at different current densities from 0.053 to 0.319 mA cm^{-2} in the potential window of 0–0.8 V. (c) The areal capacitance with various currents. (d) The high-frequency region of Nyquist impedance plot. The inset displays the Nyquist impedance plot of the wire-like SCs. (e) Performance of capacitance stability of the $NiCo_2O_4$ SC with 1000 cycles. (f) Areal energy and power density of the wire-like SCs. The inset is schematic diagram of the wire-like SC.

different stretching states was measured and shown in Fig. 4. Fig. 4a performs the CV curves of the urchin-like $NiCo_2O_4$ based SCs at different stretching states varying from 0% to 200%. It can be observed that during the stretching process, the CV curves changed slightly, which indicates the good mechanical stretchability of the wire-like SCs devices. The excellent stretchable performance results from the form of long chains of PVA molecules. The GCD profiles at different strains were displayed in Fig. 4b. The curves illustrate that the areal capacitance retains 94.65% of the pristine value at 200% strain. Fig. 4c displays the cycling performance of the device measured with 100% strain for 1000 cycles. The areal capacitance calculated from the GCD curves remains 85.77% after stretching 1000 times at the current density of 0.085 mA cm^{-2}, which proves the excellent cycling stability of the SCs. The insets present the photographs of the original device and the device under 100% stretching (from 1.5 to 3 cm). The charge transport resistances change from 20.5 to 230 Ω with stretching up to 200%, as shown in Fig. 4d. The reason of the increasing resistance can be ascribed to the slightly undesirable contact among the $NiCo_2O_4$ electrode materials during stretching.

In view of the outstanding self-healing properties of the PVA fiber, as provided in Fig. 1d, the self-healing electrochemical performances of wire-like SCs were performed in Fig. 5. From Fig. 5a, a negligible change of occlusive area is observed after four breaking/healing times, revealing the excellent self-healing stability of the SCs. Furthermore, the GCD curves of the SCs for different cutting/self-healing cycles are shown in Fig. 5b. During the cutting/self-healing process, the SC inevitably goes through vigorous operation, leading to mismatching between the broken surfaces and deviating curves for a little bit [39]. Fig. 5c exhibits the areal capacitance calculated from the GCD curves after healing for 4 cycles. 82.19% of the pristine capacitance retains after the fourth self-healing, which is much higher than the previously reported results [22]. The photographs of the original SC and after healing are displayed in Fig. 5c inset. Besides, the SEM images of healed area are presented (Fig. S4, Supplementary information). It is worth noting that the charge transport resistance is almost unchanged (from 145 to 175 Ω) after 4 cycles of cutting/healing process, as shown in Fig. 5d, which demonstrates the good concatenation of the electrode materials and good reconnection of PVA fibers.

CONCLUSIONS

In conclusion, a self-healable SC has been successfully

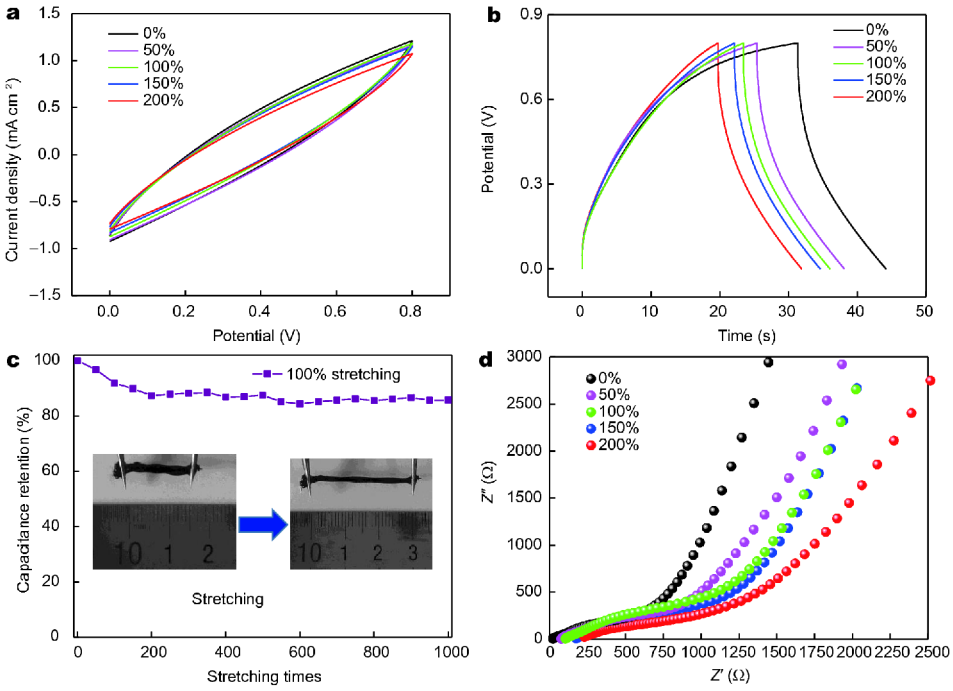

Figure 4 The stretchable properties of the wire-like SC devices. (a, b) CV curves and GCD curves under stretching from 0 to 200%. (c) Variation of capacitance stability of the 100% stretching with 1000 cycles. The insets present the photographs of the device under pristine and stretching states. (d) The Nyquist impedance plots of the as-prepared SC with various stretch.

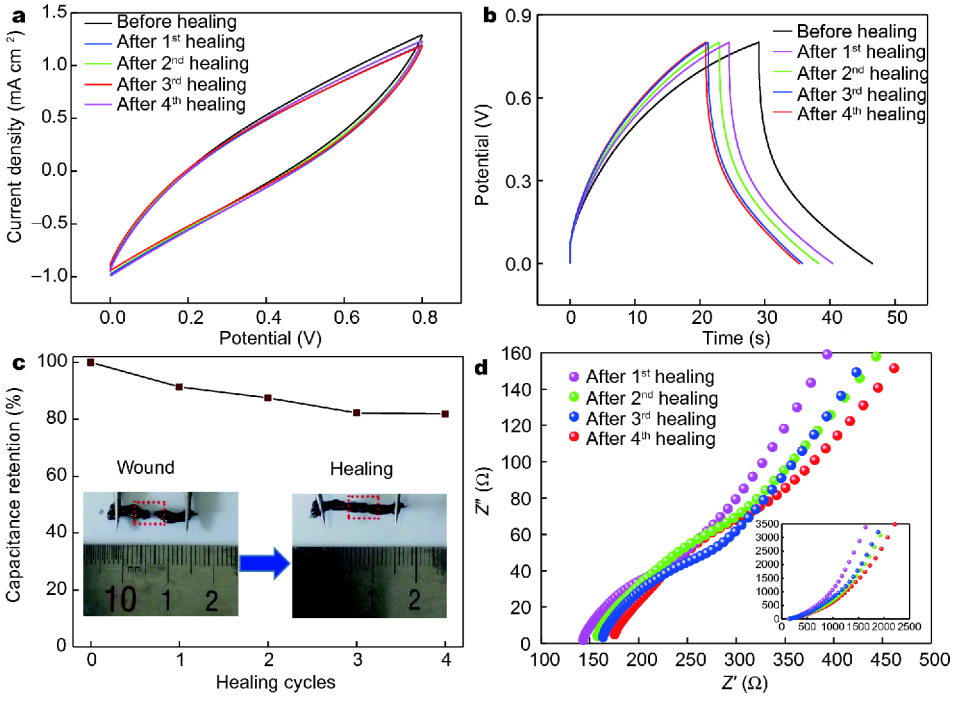

Figure 5 The self-healing properties of wire-like SC device at different cutting/self-healing cycles. (a) CV curves at the scan rate of 3.0 V s^{-1}. (b) GCD curves at the current density of 0.106 mA cm^{-2}. (c) Capacitance retention of the device after self-healing for 4 cycles. The insets show the photographs of the device under cutting and healing states. (d) The corresponding Nyquist impedance plots with different self-healing times.

fabricated by employing two twisted $NiCo_2O_4$ coated PVA fibers. The as-prepared PVA fibers possess the features of high length-diameter ratio, good stretchability, excellent ionic conductivity and outstanding self-healing ability, which paves a way for wire-like self-healing SCs and extends the lifetime of the devices. An areal capacitance of 3.88 mF cm^{-2} was obtained and the wire-like SCs show excellent cycling stability with a capacitance cycle retention of 88.23% after 1000 charge/discharge cycles. Furthermore, the assembled wire-like SCs have superior stretchability and self-healable ability. With stretching up to 200%, the areal capacitance retention rate is 94.65%, and after four damaging/healing cycles, 82.19% capacitance retains, which indicates that the wire-like SCs could be served as a promising candidate for self-healable and wearable electronic devices.

Received 8 November 2017; accepted 8 December 2017; published online 12 January 2018

1 Liu N, Ma W, Tao J, *et al.* Cable-type supercapacitors of three-dimensional cotton thread based multi-grade nanostructures for wearable energy storage. Adv Mater, 2013, 25: 4925–4931
2 Shim BS, Chen W, Doty C, *et al.* Smart electronic yarns and wearable fabrics for human biomonitoring made by carbon nanotube coating with polyelectrolytes. Nano Lett, 2008, 8: 4151–4157
3 Zhong J, Zhang Y, Zhong Q, *et al.* Fiber-based generator for wearable electronics and mobile medication. ACS Nano, 2014, 8: 6273–6280
4 Xie K, Wei B. Materials and structures for stretchable energy storage and conversion devices. Adv Mater, 2014, 26: 3592–3617
5 Xu Y, Lin Z, Huang X, *et al.* Flexible solid-state supercapacitors based on three-dimensional graphene hydrogel films. ACS Nano, 2013, 7: 4042–4049
6 Tao J, Liu N, Ma W, *et al.* Solid-state high performance flexible supercapacitors based on polypyrrole-MnO_2-carbon fiber hybrid structure. Sci Rep, 2013, 3: 2286
7 Jiang K, Wang J, Li Q, *et al.* Superaligned carbon nanotube arrays, films, and yarns: a road to applications. Adv Mater, 2011, 23: 1154–1161
8 Deng F, Lu W, Zhao H, *et al.* The properties of dry-spun carbon nanotube fibers and their interfacial shear strength in an epoxy composite. Carbon, 2011, 49: 1752–1757
9 Peng H, Jain M, Peterson DE, *et al.* Composite carbon nanotube/silica fibers with improved mechanical strengths and electrical conductivities. Small, 2008, 4: 1964–1967
10 Wang Q, Wang X, Xu J, *et al.* Flexible coaxial-type fiber supercapacitor based on $NiCo_2O_4$ nanosheets electrodes. Nano Energ, 2014, 8: 44–51
11 Kou L, Huang T, Zheng B, *et al.* Coaxial wet-spun yarn supercapacitors for high-energy density and safe wearable electronics. Nat Commun, 2014, 5: 3754
12 Zhang D, Miao M, Niu H, *et al.* Core-spun carbon nanotube yarn supercapacitors for wearable electronic textiles. ACS Nano, 2014, 8: 4571–4579
13 Jian M, Wang C, Wang Q, *et al.* Advanced carbon materials for flexible and wearable sensors. Sci China Mater, 2017, 60: 1026–1062
14 Raymundo-Piñero E, Cadek M, Wachtler M, *et al.* Carbon nanotubes as nanotexturing agents for high power supercapacitors based on seaweed carbons. ChemSusChem, 2011, 4: 943–949
15 Wang X, Lu X, Liu B, *et al.* Flexible energy-storage devices: design consideration and recent progress. Adv Mater, 2014, 26: 4763–4782
16 Huang L, Yi N, Wu Y, *et al.* Multichannel and repeatable self-healing of mechanical enhanced graphene-thermoplastic polyurethane composites. Adv Mater, 2013, 25: 2224–2228
17 Hager MD, Greil P, Leyens C, *et al.* Self-healing materials. Adv Mater, 2010, 22: 5424–5430
18 Huang Y, Zhu M, Huang Y, *et al.* Multifunctional energy storage and conversion devices. Adv Mater, 2016, 28: 8344–8364
19 Sun H, You X, Jiang Y, *et al.* Self-healable electrically conducting wires for wearable microelectronics. Angew Chem Int Ed, 2014, 53: 9526–9531
20 Xue Q, Sun J, Huang Y, *et al.* Recent progress on flexible and wearable supercapacitors. Small, 2017, 13: 1701827
21 Huang Y, Zhong M, Shi F, *et al.* An intrinsically stretchable and compressible supercapacitor containing a polyacrylamide hydrogel electrolyte. Angew Chem Int Ed, 2017, 56: 9141–9145
22 Wang S, Liu N, Su J, *et al.* Highly stretchable and self-healable supercapacitor with reduced graphene oxide based fiber springs. ACS Nano, 2017, 11: 2066–2074
23 Wang H, Zhu B, Jiang W, *et al.* A mechanically and electrically self-healing supercapacitor. Adv Mater, 2014, 26: 3638–3643
24 Wang K, Zhang X, Li C, *et al.* Chemically crosslinked hydrogel film leads to integrated flexible supercapacitors with superior performance. Adv Mater, 2015, 27: 7451–7457
25 Wang DW, Li F, Liu M, *et al.* 3D aperiodic hierarchical porous graphitic carbon material for high-rate electrochemical capacitive energy storage. Angew Chem Int Ed, 2008, 47: 373–376
26 Yuan C, Zhang X, Su L, *et al.* Facile synthesis and self-assembly of hierarchical porous NiO nano/micro spherical superstructures for high performance supercapacitors. J Mater Chem, 2009, 19: 5772–5777
27 Wu T, Li J, Hou L, *et al.* Uniform urchin-like nickel cobaltite microspherical superstructures constructed by one-dimension nanowires and their application for electrochemical capacitors. Electrochim Acta, 2012, 81: 172–178
28 Li L, Lou Z, Han W, *et al.* Flexible in-plane microsupercapacitors with electrospun $NiFe_2O_4$ nanofibers for portable sensing applications. Nanoscale, 2016, 8: 14986–14991
29 Wu H, Jiang K, Gu S, *et al.* Two-dimensional $Ni(OH)_2$ nanoplates for flexible on-chip microsupercapacitors. Nano Res, 2015, 8: 3544–3552
30 Ai Y, Lou Z, Li L, *et al.* Meters-long flexible $CoNiO_2$-nanowires@carbon-fibers based wire-supercapacitors for wearable electronics. Adv Mater Technol, 2016, 1: 1600142
31 Wang Z, Tao F, Pan Q. A self-healable polyvinyl alcohol-based hydrogel electrolyte for smart electrochemical capacitors. J Mater Chem A, 2016, 4: 17732–17739
32 Sun K, Ran F, Zhao G, *et al.* High energy density of quasi-solid-state supercapacitor based on redox-mediated gel polymer electrolyte. RSC Adv, 2016, 6: 55225–55232
33 Huang Y, Huang Y, Zhu M, *et al.* Magnetic-assisted, self-healable, yarn-based supercapacitor. ACS Nano, 2015, 9: 6242–6251
34 Wang Q, Wang X, Liu B, *et al.* $NiCo_2O_4$ nanowire arrays supported

on Ni foam for high-performance flexible all-solid-state supercapacitors. J Mater Chem A, 2012, 1: 2468–2473
35 Wang Q, Liu B, Wang X, *et al.* Morphology evolution of urchin-like $NiCo_2O_4$ nanostructures and their applications as psuedocapacitors and photoelectrochemical cells. J Mater Chem, 2012, 22: 21647–21653
36 Bae J, Song MK, Park YJ, *et al.* Fiber supercapacitors made of nanowire-fiber hybrid structures for wearable/flexible energy storage. Angew Chem Int Ed, 2011, 50: 1683–1687
37 Li L, Chen C, Xie J, *et al.* The preparation of carbon nanotube/MnO_2 composite fiber and its application to flexible micro-supercapacitor. J Nanomaterials, 2013, 2013: 1–5
38 Ren J, Li L, Chen C, *et al.* Twisting carbon nanotube fibers for both wire-shaped micro-supercapacitor and micro-battery. Adv Mater, 2013, 25: 1155–1159
39 Huang Y, Zhong M, Huang Y, *et al.* A self-healable and highly stretchable supercapacitor based on a dual crosslinked polyelectrolyte. Nat Commun, 2015, 6: 10310

Acknowledgements This work was supported by the National Natural Science Foundation of China (61625404 and 61504136), Beijing Natural Science Foundation (4162062), and the Key Research Program of Frontiers Sciences, CAS (QYZDY-SSW-JSC004).

Author contributions Jia R and Li L contributed equally to this work. The paper was written through contributions of all authors. All authors have given approval to the final version of the paper.

Conflict of interest The authors declare no conflict of interest.

Supplementary information Supporting data are available in the online version of the paper.

Rui Jia received her BE degree from Huaqiao University in 2015. Now she is a master student at the College of Chemistry and Chemical Engineering, Qingdao University. Her research interest focuses on flexible supercapacitors.

La Li received her BSc degree from Jilin University in 2013. She is a PhD candidate at the College of Physics, Jilin University, China. Her research interests mainly focus on flexible micro-supercapacitors and self-powered integrated devices.

Zhaojun Chen received his BE degree and MSc degree from Qingdao University in 2000 and 2005, respectively, and received his PhD degree from China University of Petroleum in 2015. He is currently an Associate Professor at Qingdao University. His current research focuses on the design and synthesis of novel nanostructure materials for applications in supercapacitors, biomedical materials and catalysts.

Guozhen Shen received his BSc degree in 1999 from Anhui Normal University and PhD degree in 2003 from the University of Science and Technology of China. From 2004 to 2009, he conducted his research in Hanyang University (Korea), National Institute for Materials Science (Japan), University of Southern California (USA) and Huazhong University of Science and technology. He joined the Institute of Semiconductors, Chinese Academy of Sciences as a professor in 2013. His current research focuses on flexible electronics and printable electronics, including transistors, photodetectors, sensors and flexible energy-storage devices.

两根$NiCo_2O_4$涂覆的聚乙烯醇水凝胶纤维构建线状可自愈超级电容器

贾蕊[1,2†], 李腊[2†], 艾远飞[2], 杜辉[1], 张晓东[1], 陈照军[1*], 沈国震[2,3*]

摘要 线状超级电容器因其轻量、柔性及可编织性的特点引起了广泛关注. 如何延长超级电容器的使用寿命仍然是当前所面临的一个挑战. 本文报道了一种新型的可拉伸和自愈的线状超级电容器. 首先将两根由海胆状$NiCo_2O_4$纳米材料包裹的聚乙烯醇/氢氧化钾(PVA/KOH)水凝胶缠绕在一起, 进而形成一个完整的超级电容器. 值得注意的是, PVA水凝胶可以很容易地用一个比较小的拉力(12.51 kPa)实现300%的形变量. 这一结果优于之前报道的以350 kPa的拉力拉伸到300%应变的聚氨酯. 此外, 该线状超级电容器表现出良好的电化学性能. 在电流密度为0.053 mA cm^{-2} 时面积比电容为3.88 mF cm^{-2}, 并且在1000次充放电后仍有88.23%的剩余面积比电容, 显示了良好的循环稳定性. 此外, 在四次切断/自愈后电容保留量仍有82.19%. 这项工作将会为下一代自愈和可穿戴设备提供一种新的设计方案.

